INVESTIGATION OF FLOW PROFILE IN OPEN CHANNELS USING CFD

B. K. Gandhi
Professor, Department of Mechanical and Industrial Engineering,
Indian Institute of Technology Roorkee,
E-mail: bhupendragandhi@gmail.com,
Phone: +91-1332-285544, Fax: +91-1332-285665, 273560

H.K. Verma
Professor, Department of Electrical Engineering,
Indian Institute of Technology Roorkee,
E-mail: hkvfee@gmail.com,
Phone: +91-1332-285588, Fax: +91-1332-273560

Boby Abraham
Senior System Engineer,
IBM India Pvt. Limited, Bangalore,
E-mail: baysayoor@yahoo.co.in

ABSTRACT

Accuracy of the efficiency measurement of a hydro-electric generating unit depends on the measurement uncertainties of discharge, head and power, where the uncertainties in the measurement of discharge predominate. The discharge through open channel flow is often evaluated by velocity-area integration method from the measurement of velocity at discrete locations in the measuring section. The variation of velocity along horizontal and vertical directions is thus very important to decide the locations of velocity sensors, like propeller current meters or acoustic transducers of an ultrasonic transit-time flowmeter.

An effort has been made through the present investigation to determine the velocity profiles in both the directions under different real flow conditions, as ideal flow conditions rarely exist in the field. 'Fluent', a commercial computational fluid dynamics (CFD) code, has been used to numerically model various situations. The validation of CFD model has been carried out by determining the actual velocity profile with acoustic Doppler current profiler (ADCP), a non-intrusive instrument. Effects of bed slope, upstream bend and a convergence / divergence of channel width on velocity profile have been investigated and discussed. It is observed that the actual velocity profile differs from the normal profile due to non-existence of ideal flow conditions, and this should be taken care during the planning of measurement of velocity by any method in the flow section to evaluate the discharge using velocity-area integration technique.

Keywords: Acoustic Doppler current profiler (ADCP), Computational fluid dynamics (CFD), Discharge measurement, Flow-velocity profile, Flow sensor, Open channel, Propeller current meter, Ultrasonic transit-time flowmeter, Velocity-area integration.

1. INTRODUCTION

The measurement of discharge through a hydro-turbine needs velocity measurement at a number of points in the measuring section and, subsequently, application of an appropriate integration technique [1]. In many cases, the discharge measurement needs to be done in an open channel at either the headrace or the tailrace of the hydro-electric power station. An open channel always has two sides and a bottom where flow velocity has to satisfy no-slip condition. Therefore, even a straight channel has a three-dimensional velocity distribution with complex velocity profiles due to turbulence. The maximum velocity is seen typically at about 20% of the depth below the free surface in the middle of channel width [2]. In very broad shallow channels, the maximum velocity is near the surface and the velocity profile is nearly logarithmic from the bottom to the free surface. In non-circular channels, a secondary flow also exists, which intensifies in case the channel is curved or meandered.

The ideal flow conditions generally do not exist in real situations, especially in small hydro electric power stations. If discharge measurement has to be done in an unsatisfactory situation, large measurement errors may occur. The irregularity of the open channel is one of the major factors that increase the

measurement uncertainty. The velocity profiles developed in various geometries of open channel are found to be very complex, such that the accurate measurement of these profiles becomes a tedious and challenging job [3]. Propeller current-meters and ultrasonic (acoustic) transit-time flow-meter are the two methods recommended to be used in such situations [1]. However, the systematic error in either method can be reduced considerably by locating the current meters/ acoustic transducers appropriately. This in turn requires knowledge of the flow-velocity profile in the open channel.

Mathematical models of the velocity profile in circular pipes are available [3] and have been used for determining the most appropriate locations of current meters/acoustic transducers for minimizing the systematic error in discharge measurement in circular penstocks. However, to the best of authors' knowledge, such mathematical models are not available for open channels. In the open channel flow, the velocity distribution along the vertical direction (depth) is theoretically represented by a logarithmic function of the depth of flow [4]. It is very difficult to describe the velocity distribution along the width theoretically. However, some of the investigators have proposed empirical equations for the velocity distribution based on experimental and field data [5-8].

In the present work, an effort has been made to investigate the velocity profiles for various open-channel geometries using a commercial computational fluid dynamics (CFD) code, namely FLUENT. The CFD model developed for a real open-channel was first validated by comparing the velocity profile obtained from it with that obtained by actual measurement in the same channel using an acoustic Doppler current profiler (ADCP). The CFD model has been the used to analyze the effects of upstream bend, divergence/convergence of channel width and bed slope, and to study the variations in velocity profiles along the horizontal and vertical directions. The results are presented in this paper. The CFD analysis has been carried out for as many as six different geometries and the results are discussed here. All the geometries are modeled with similar operating and boundary conditions.

2. NUMERICAL MODEL

A CFD code, namely FLUENT [9], has been used in the present work for analysis of open channel flow. It is a state-of-art software package for analyzing fluid flow and heat transfer problems involving complex geometries. The numerical scheme employed belongs to the finite-volume group and adopts integral form of the conservation equations. The solution domain is subdivided into a finite number of contiguous control volumes and conservation equations are applied to each control volume. Surface and volume integrals are approximated using suitable quadrature formulae.

The open channel flow is modeled in FLUENT using volume of fluid (VoF) formulations. The flow involves existence of a free surface between the flowing fluid and the atmospheric air above it. The flow is generally governed by the forces of gravity and inertia. In VoF model, a single set of momentum equations is solved for two or more immiscible fluids by tracking the volume fraction of each of the fluids throughout the domain. The mathematical formulation adopted is described briefly below.

The tracking of interface between the two phases is accomplished by the solution of continuity equations for their volume fractions. For phase '2' the equation for steady flow can be written as,

$$\nabla (\alpha_2 \rho_2 \vec{v}_2) = S_{\alpha_2} + \sum_{p=1}^{2} (\dot{m}_{p2} - \dot{m}_{2p}) \quad \ldots\ldots \quad (1)$$

where

α_q is the volume fraction of 2nd phase fluid in primary phase '1',
ρ_2 is mass density of phase '2' (kg m^{-3}),
$\vec{v}_2$ is mean velocity vector of phase '2' (m),
S_{α_2} is the rate of phase '2' mass per unit volume added externally to primary phase '1' (kg m^{-3} s^{-1}),
$\dot{m}_{p2}$ is the rate of mass transfer from phase 'p' to phase '2' (kg m^{-3} s^{-1}), and
$\dot{m}_{2p}$ is the rate of mass transfer from phase 'p' to phase 'p' (kg m^{-3} s^{-1})

The volume fraction-averaged density and viscosity are computed for each cell as below:

$$\rho = \sum \alpha_A \rho_A \quad \ldots\ldots\ldots \quad (2)$$

A single momentum equation is then solved throughout the domain, and the resulting velocity field is shared among the phases.

Conservations of momentum for the i^{th} direction in an inertial reference frame is written as

$$\frac{\partial}{\partial x_i}\left(\rho u_i u_j\right) = -\frac{\partial p}{\partial x_i} + \frac{\partial \tau_{ij}}{\partial x_i} + \rho g_i + F_i \quad \text{..... (3)}$$

where

x_j is longitudinal co-ordinate in j^{th} direction (m),
u_j is mean longitudinal velocity in j^{th} direction (m s^{-1}),
p is static pressure (N m^{-2}),
ρg_i is body force per unit volume in i^{th} direction (N m^{-3}),
τ_{ij} is shear stress tensor (N m^{-2}), and
F_i is external force per unit volume (N m^{-3})

The shear stress tensor is given by

$$\tau_{ij} = \left[\frac{\partial u_i}{\partial x_i} + \frac{\partial u_j}{\partial x_i}\right] - \frac{2}{3}\mu \frac{\partial u_i}{\partial x_i}\delta_{ij} + \left(\tau_{ij}\right)_t \quad \text{..... (4)}$$

where

μ is effective dynamic viscosity (Ns m^{-2}),
δ_{ij} is Kroneker delta function, and
$(\tau_{i,j})_t$ is Reynolds stress tensor (N m^{-2})

The second term on the right hand side of equation (4) is the effect of volume dilation. For calculating the pressure, the method is derived from the SIMPLE algorithm of Patankar [10]. The geometry taken for CFD analysis configures open channel of different cross-sections with water flowing through the channel and free surface exposed to atmospheric air. 'Pressure inlet' and 'pressure outlet' are given as inlet and outlet boundary conditions. The water flow and free surface slope in the domain are obtained by the bed levels of the channel for steady-state condition.

3. TURBULENCE MODEL USED

Small high-frequency fluctuations are present even in steady flow and, to account for these, time averaging procedure is employed, which results in additional terms. These additional terms need to be expressed as calculable quantities for closure solutions. The standard κ-ε model has been used in the present case. It is a semi-empirical model based on model transport equations for the turbulent-kinetic energy 'κ' and its dissipation rate 'ε', and is expressed by the following equations:

$$\rho u_i \frac{\partial k}{\partial x_i} = \frac{\partial}{\partial x_i}\left[\left(\mu + \frac{\mu_t}{\sigma_k}\right)\frac{\partial k}{\partial x_i}\right] + G_k + G_b - \rho\varepsilon - Y_m \quad \text{..... (5)}$$

$$\rho u_i \frac{\partial \varepsilon}{\partial x_i} = \frac{\partial}{\partial x_i}\left[\left(\mu + \frac{\mu_t}{\sigma_\varepsilon}\right)\frac{\partial \varepsilon}{\partial x_i}\right] + C_{1\varepsilon}\frac{\varepsilon}{k}\left(G_k + C_{3\varepsilon}G_b\right) - C_{2\varepsilon}\frac{\rho\varepsilon^2}{k} \quad \text{..... (6)}$$

where

κ is turbulent kinetic energy (N m),
μ_t is eddy/turbulent viscosity (Ns m^{-2}),
σ_κ is turbulent Prandlte number for κ,
σ_ε is turbulent Prandlte number for ε,
G_b is generations term (buoyancy),
Gκ is generations term (kinetic),
ε is turbulence dissipation rate ($Nm^2\,kg^{-1}$),
Y_m is fluctuating dilation, and
$C_{1\varepsilon}$, $C_{2\varepsilon}$ and $C_{3\varepsilon}$ are turbulence model constants

Here G_κ represents the generation of turbulent kinetic energy due to the mean velocity gradient calculated from,

$$G_k = \mu_t S^2 \quad \text{..... (7)}$$

where 'S' represents the modulus of mean rate of stress and is calculated from,

$$S = \sqrt{2\,S_{ij}\,S_{ij}} \quad \text{..... (8)}$$

The mean stress rate, S_{ij}, is given by

$$S_{ij} = \frac{1}{2}\left[\frac{\partial u_i}{\partial x_j} + \frac{\partial u_j}{\partial x_i}\right] \quad \text{..... (9)}$$

and G_b represents generation of turbulent kinetic energy due to buoyancy which has been taken as zero for no temperature gradient. The eddy or turbulent viscosity, μ_t, is computed using the equation

$$\mu_t = \rho C_\mu \frac{\kappa^2}{\varepsilon} \quad \text{..... (10)}$$

The values of model constants are taken as: $C_{1\varepsilon} = 1.44$, $C_{2\varepsilon} = 1.92$, $C_\mu = 0.09$, $\sigma_\kappa = 1.0$ and $\sigma_\varepsilon = 1.3$ [9]. As G_b has been taken zero, the value of $C_{3\varepsilon}$ is not needed.

4. Validation of CFD Model

For validation of CFD simulation, the velocity profile across the width of a channel is measured by an acoustic Doppler current profiler (ADCP) and compared with the numerical results. A long straight water conveying canal, with a well defined cross section and flowing near Roorkee (India), has been selected for this purpose. The canal is cement-lined with left wall vertical and the right wall being tapered. The width of the channel is 5.2 m and 4 m at the top and bottom, respectively, with a 30.96° taper angle for right wall. The channel width is divided into cells of 0.1 m size for measurement of average velocity at the centre of each cell by ADCP. For CFD simulation, the flow domain is initially discretized with hexahedral elements of face length equals to 0.01 m, 0.005 m and 0.0025 m. The results with 0.005 m and 0.0025 m show variations within 0.5% only and, therefore, a mesh spacing of 0.005 m is selected for further analysis. Flow is assumed to be steady, turbulent and three-dimensional.

The average velocity profiles along the width of the channel obtained from ADCP measurement and CFD simulation, respectively, are shown in Fig. 1. It is seen that the two profiles are similar in nature and are lying very close to each other. The values of discharge evaluated from the two velocity profiles using velocity-area integration method are as under:

Discharge from ADCP measurement data = 1.621 m^3/s

Discharge from CFD simulation data = 1.604 m^3/s

Percent difference in the two discharge rates is only 1.05 %, which shows that the CFD simulation compares well with results of the measurement made with ADCP. Consequently, the CFD model developed above has been used in further analysis.

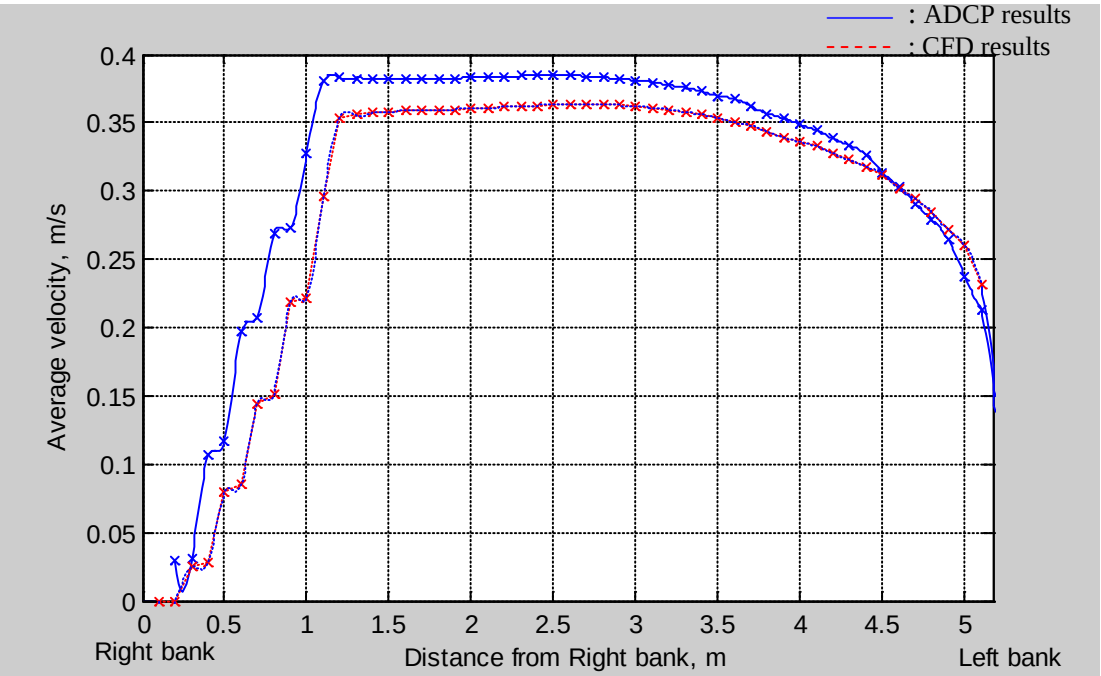

Fig. 1: Average velocity profiles obtained from ADCP measurement and CFD simulation

5. RESULTS AND DISCUSSION

The velocity profiles for various open channel geometries have been simulated by VoF model using the CFD code, FLUENT. The details of each channel geometry and site conditions are given in Table 1. The development of flow in the channel for the six geometries has been analyzed by plotting velocity contours at different flow-sections along the flow direction in the channel and are presented in Fig. 2. For each case, that is geometry of channel, the velocity profiles have been plotted at different flow sections to observe the position of maximum velocity and the variations in the profile.

Table 1: Details of different case studies and results of numerical solution

Sr. No.	Case details	Channel geometry details	Figure No.
1	Rectangular Open channel with Small Slope (Profile P1)	Depth = 2 m, Width = 4 m, Length = 15 m, Slope = 1/75	2a
2	Rectangular Open Channel with Medium Slope (Profile P2)	Depth = 2 m, Width = 4 m, Length = 15 m, Slope = 1/30	2b
3	Rectangular Open Channel with Large Slope (Profile P3)	Depth = 2 m, Width = 4 m, Length = 15 m, Slope = 1/10	2c
4	Rectangular Open Channel with 90˚ Bend (Profile B1)	Depth = 2 m, Width = 4 m, Length = 15 m, Slope = 1/75, Bend = 90˚	2d
5	Rectangular Open Channel with Divergence (Profile D1)	Depth = 2 m, Divergence length = 4 m, Width before divergence = 3 m, Width after divergence = 6 m, Divergence angle = 20.56 Total length = 15 m, Slope = 1/75	2e
6	Rectangular Open Channel with Convergence (Profile C1)	Depth = 2 m, Convergence length = 4 m, Width before convergence = 6 m, Width after convergence = 3 m, Convergence angle = 20.56, Total length = 15 m, Slope = 1/75	2f

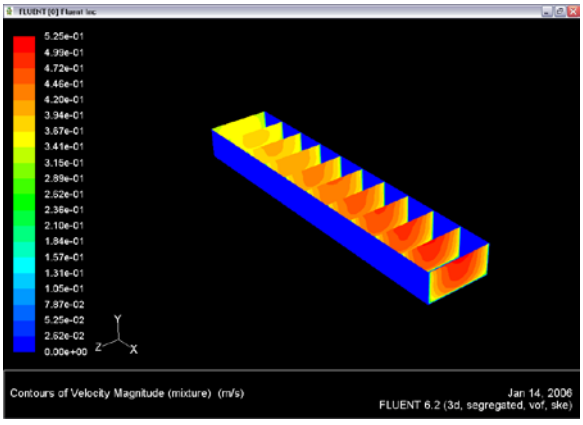

(a) Profile P1

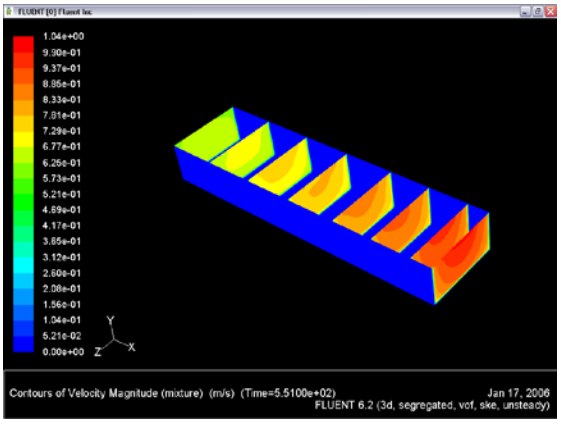

(b) Profile P2

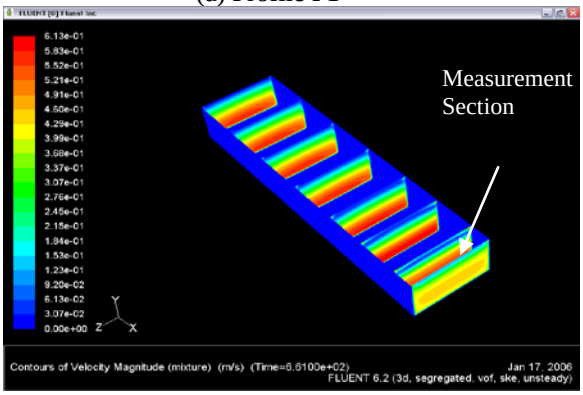

(c) Profile P3

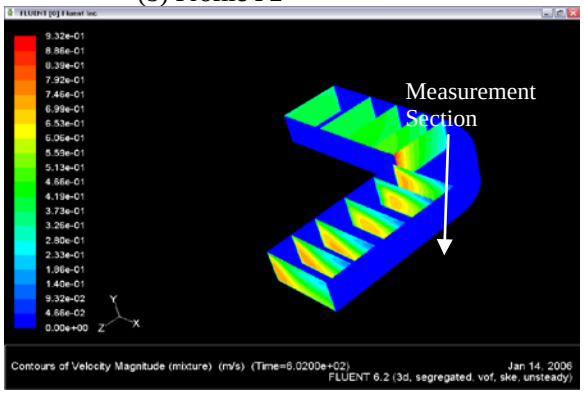

(d) Profile B1

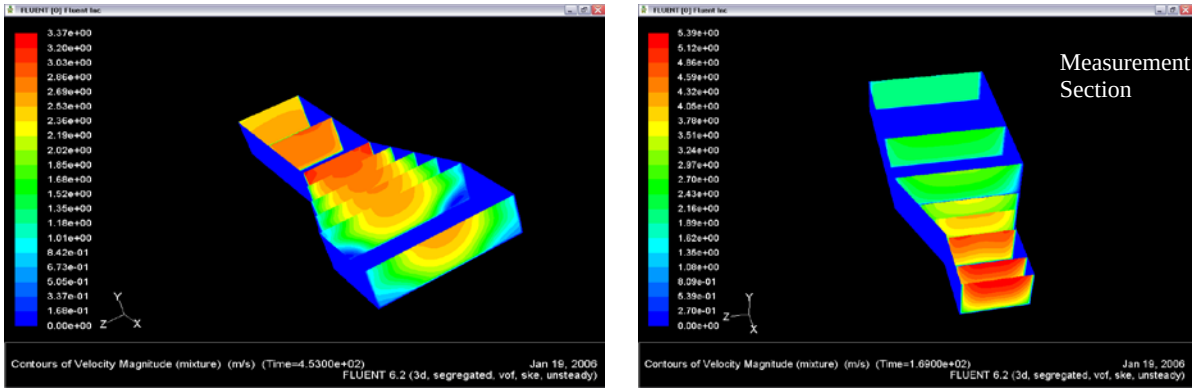

(e) Profile D1 (f) Profile C1

Fig. 2: Simulation of flow in open channel of different geometries

The effects of (i) bed slope, (ii) 90^0-bend and (iii) divergence and convergence are discussed below on the basis of the results of CFD simulation:

(i) Effect of Bed Slope

The velocity profiles for three different bed slopes namely 1/75, 1/30 and 1/10, have been plotted in Fig. 3. It is seen that as the bed slope increases, the maximum velocity (for vertical profile) shifts towards the bed side. This may be attributed to accelerating flow in the channel. The horizontal profile also becomes more flat as the bed slope increases, whereas a small bed slope results in a maximum velocity in the mid-section of the channel.

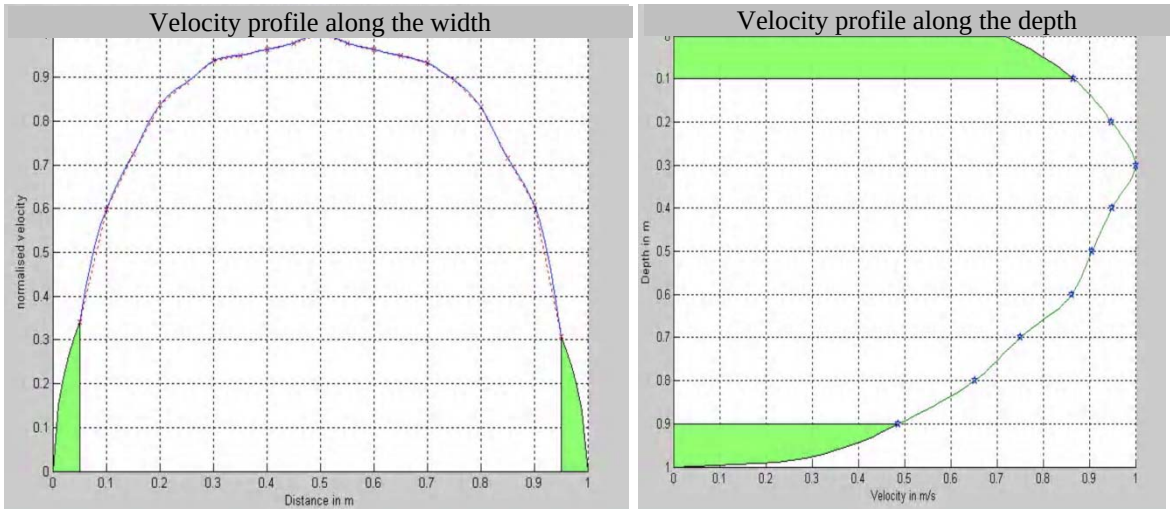

(a) Velocity profiles along horizontal and vertical directions for a bed slope of 1/75

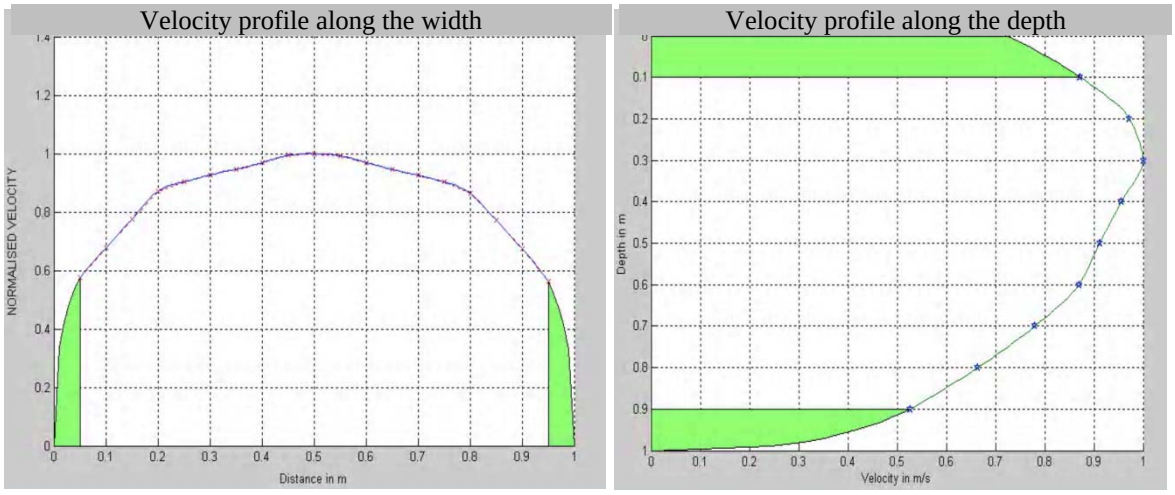

(b) Velocity profiles along horizontal and vertical directions for a bed slope of 1/30

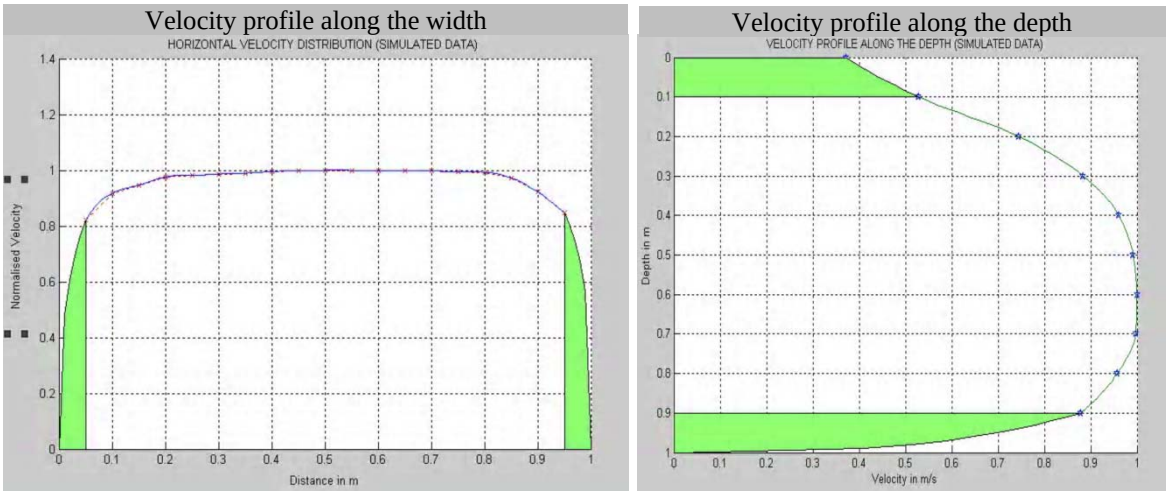

(c) Velocity profiles along horizontal and vertical directions for a bed slope of 1/10

Fig. 3: Effect of bed slope on velocity profile

(ii) Effect of 90º-Bend

An upstream bend in the channel is another major factor affecting the velocity profile as shown in Fig. 4. The vertical velocity profile becomes almost flat from mid-height to 20% below the free surface. The effect is more pronounced in the velocity profile along horizontal direction due to centrifugal effect, which becomes asymmetric in this case.

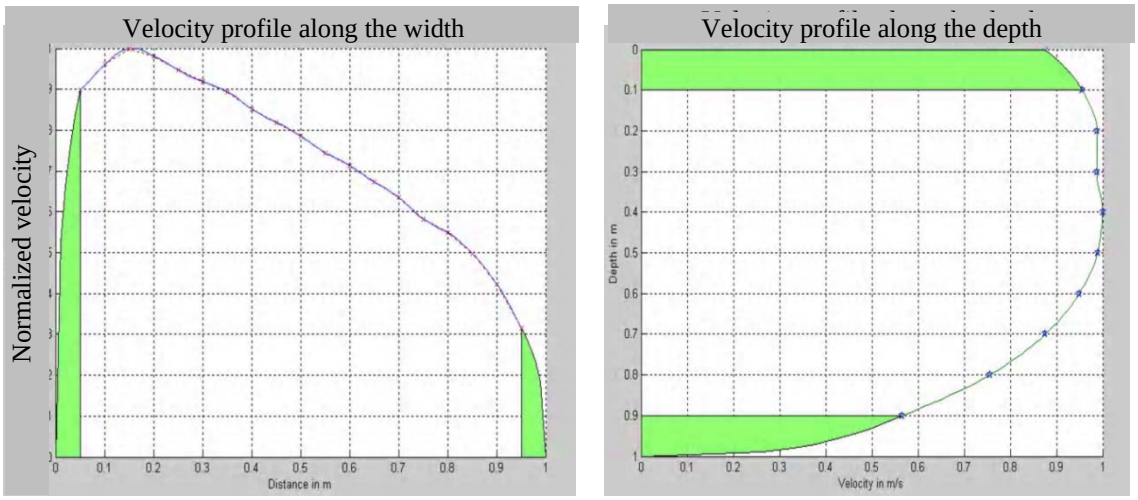

Fig. 4: Velocity profiles along horizontal and vertical directions for upstream 90º bend

(iii) Effect of Divergence and Convergence

Velocity profile is considerably affected by a change in the width of the channel. The effect of divergence and convergence due to change in channel width before the measuring section is shown in Fig. 5. It is seen that the maximum velocity occurs 20% below the free surface or at the free surface in case of divergence and convergence, respectively. The change in velocity profile along horizontal direction is totally inverse in the two cases. In case of divergence before the measuring section, high velocities are observed in the middle of the width and the velocity gradient along the channel width is very large; Fig. 5(a). However, in case of convergence before the measuring section, the velocity profile does not have very large gradients and the maximum velocity occurs at two locations equidistant from the mid point towards the wall; Fig. 5(b).

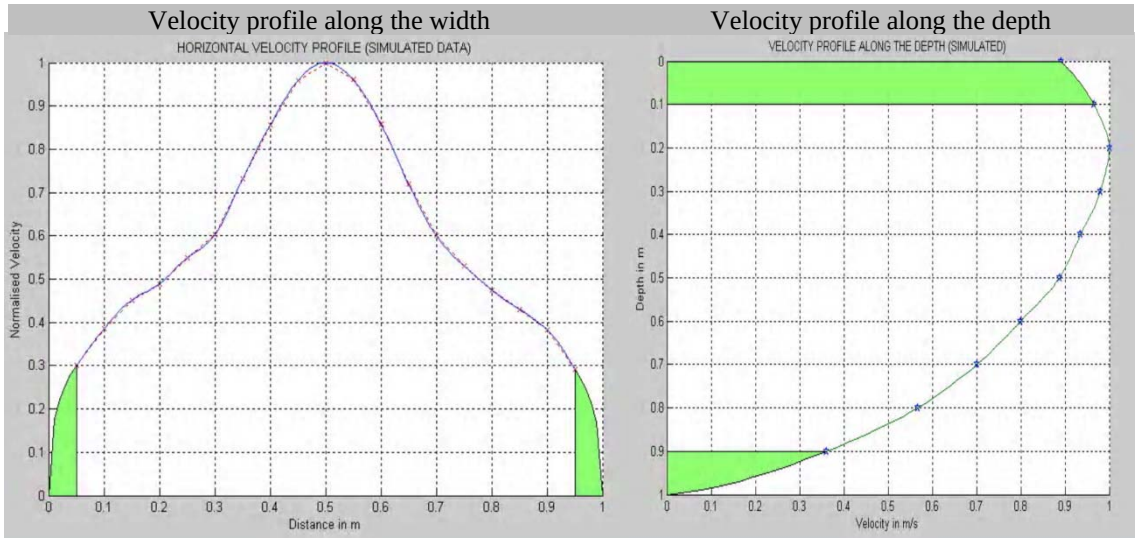

(a) Velocity profiles along horizontal and vertical directions for divergence before the measuring section

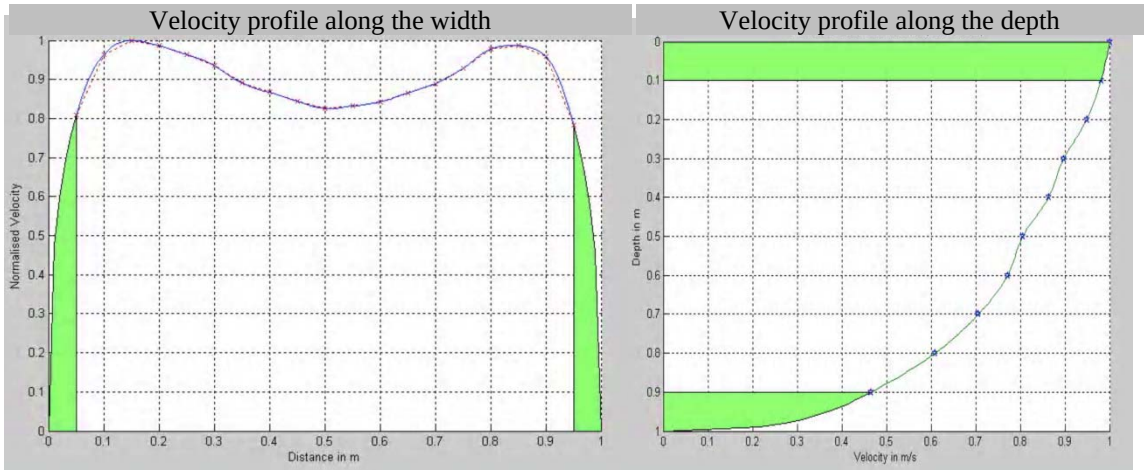

(b) Velocity profiles along horizontal and vertical directions for convergence before the measuring section

Fig. 5: Effect of divergence and convergence on velocity profiles

6. CONCLUSIONS

The flow-velocity profile in rectangular open channels has been numerically modeled. The CFD model has been validated by comparing the results with actual measurement carried out with ADCP.

The proposed numerical modeling can be used for determining the optimum number and locations of flow sensors (propeller current meters or transducers of ultrasonic transit-time flowmeter, as the case may be) for the measurement of discharge in a given open channel. This in particular is very useful in determining hydraulic efficiency of hydro-dynamic machines, where the accuracy requirement is very stringent.

The CFD model can be expanded to include the effects of silt and larger floating bodies. Trapezoidal open channels are also frequently used for feeding water to power stations, and modeling of such open channels would be, therefore, also be useful for further studies.

REFERENCES

[1] IEC-60041, “Field acceptance tests to determine the hydraulic performance of hydraulic turbines, storage pumps and pump turbines”, 1991.

[2] White, F. M., “Fluid Mechanics”, McGraw-Hill Publication, Fifth edition, 2003.

[3] Salami L.A., “On velocity-area methods for asymmetric profiles”, University of Southampton Interim Report V, 1972.

[4] Schlichting, H., “Boundary Layer Theory”, McGraw Hill, 1979.

[5] Sooky, A. A., “Longitudinal dispersion in Open Channels”, Journal of Hydraulic Division of American Society of Civil Engineering, Engineering Vol. 95, No. 4, 1969, pp. 1327-1346.

[6] Bogle, G. V., “Stream Velocity Profiles and Longitudinal Dispersion”, Journal of Hydraulic Engineering-Trans ASCE, Vol. 123, No. 9, 1997, pp. 816-820.

[7] Deng, Z., Singh, V. P. and Bengtsson, L., “Longitudinal Dispersion Coefficient in Straight Rivers”, Journal of Hydraulic Engineering-Trans ASCE, Vol. 127, No. 1, 20041 pp. 919-927.

[8] Seo, Won II and Baek, K.O., “Estimation of the longitudinal dispersion coefficient using the velocity profiles in natural streams”, Journal of Hydraulic Engineering-Trans ASCE, Vol. 130, No. 3, 2004, pp. 227-236.

[9] Fluent 6.2 User’s Guide, Fluent Inc., January 2005.

[10] Patankar, S.V., “Numerical Heat Transformer and Fluid Flow”, Hemisphere Publishing Corporation, New York, 1980.